A new difunctional copper nanocluster surface molecular imprinting polymethacrylic acid probe for ultratrace trichlorophenol based-in situ generated nanogold SPR effects

Li Lin[a,b], Aihui Liang[a,b], Guiqing Wen[a,b,*], Zhiliang Jiang[a,b,*]

[a]Key Laboratory of Ecology of Rare and Endangered Species and Environmental Protection (Guangxi Normal University), Ministry of Education, Guilin 541004, China.

[b]Guangxi Key Laboratory of Environmental Pollution Control Theory and Technology, Guilin 541004, China.

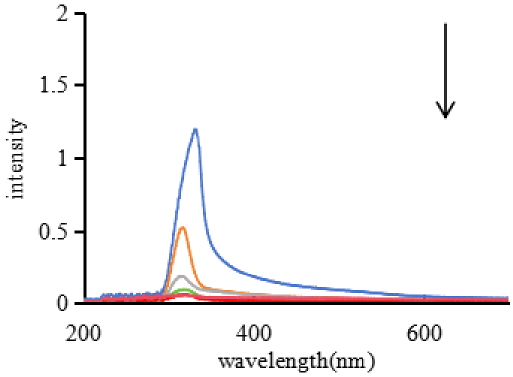

Fig.S1 UV spectra of the supernatant after CuNC@MIP elution

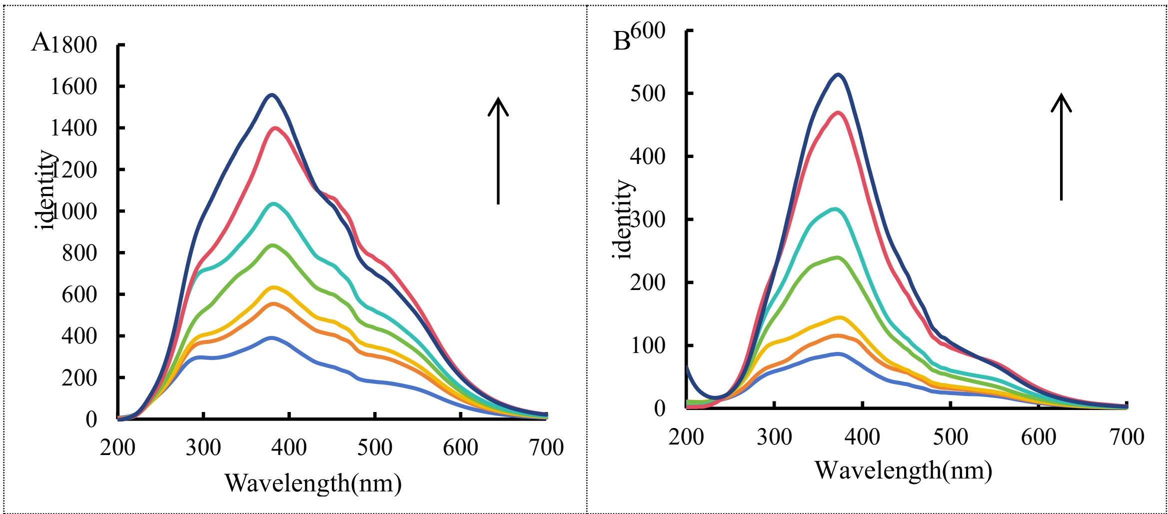

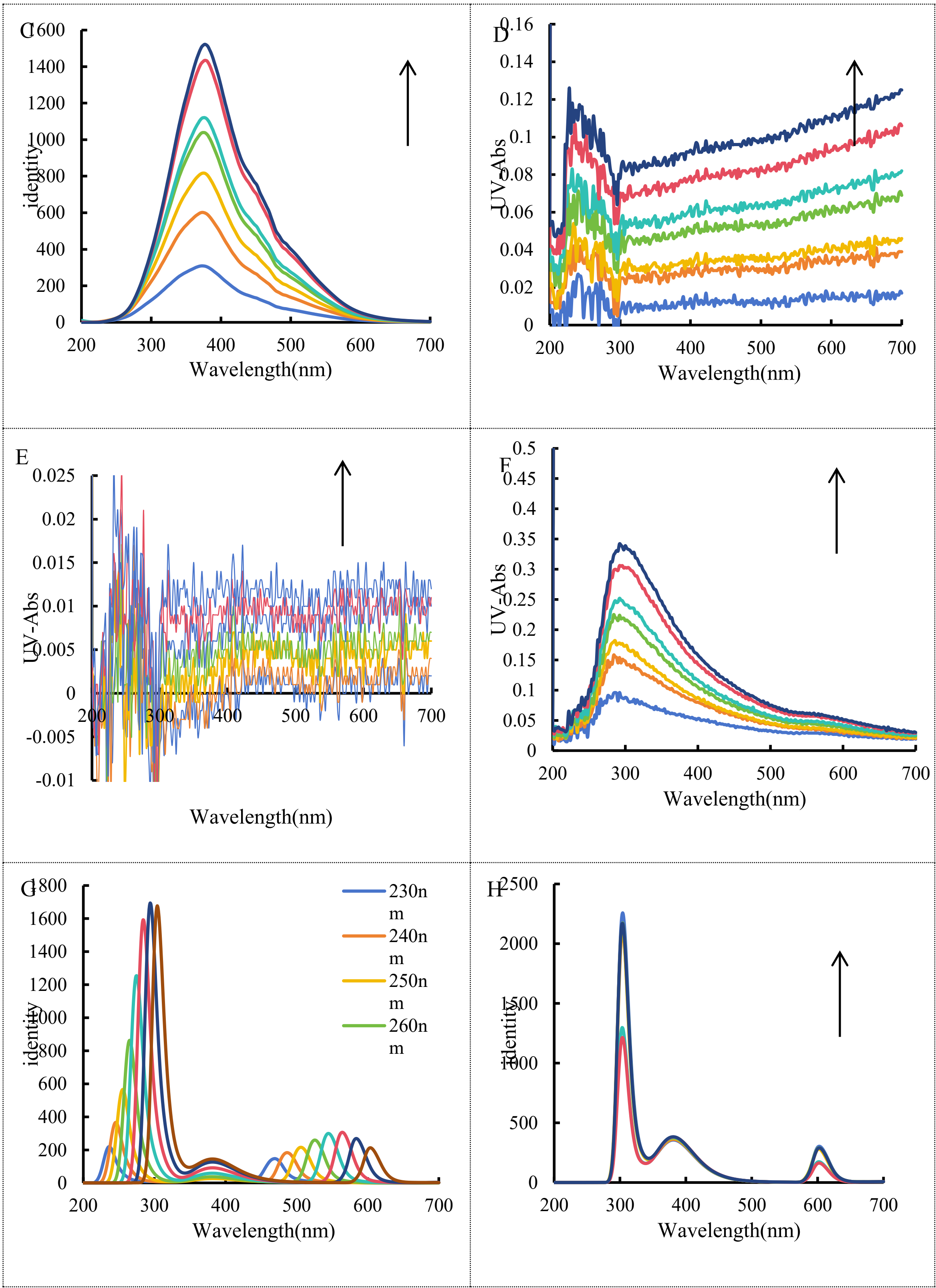
C
identity
Wavelength(nm)
D
UV-Abs
Wavelength(nm)
E
UV-Abs
Wavelength(nm)
F
UV-Abs
Wavelength(nm)
G
identity
230nm
240nm
250nm
260nm
Wavelength(nm)
H
identity
Wavelength(nm)

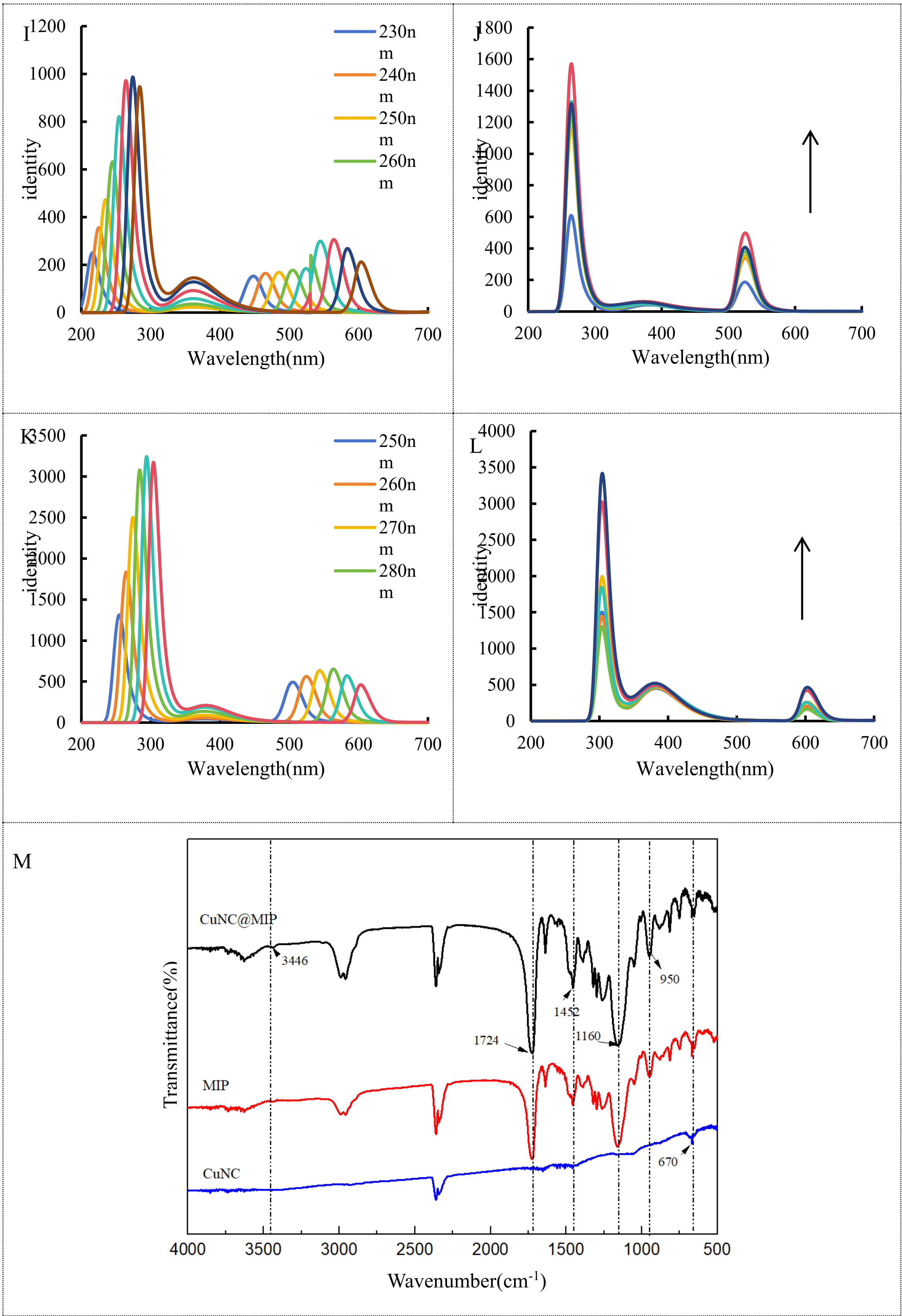

Fig. S2 Spectra of CuNC@MIP/MIP/CuNC

A: RRS spectra of (0.001,0.0025,0.0035,0.005,0.006,0.0075,0.01) g/L CuNC@MIP, B: RRS spectra of (0.001,0.0025,0.0035,0.005,0.006,0.0075,0.01) g/L MIP, C: RRS spectra of (0.0333,0.08325,0.11655,0.1665,0.1998,0.24975,0.333) mmol/L CuNC, D: Abs spectra of

(0.01,0.025,0.035,0.05,0.06,0.075,0.1) g/L CuNC@MIP, E:Abs spectra of (0.01,0.025,0.035,0.05,0.06,0.075,0.1) g/L MIP, F: Abs spectra of (0.0333,0.08325,0.11655,0.1665,0.1998,0.24975,0.333) mmol/L CuNC, G: fluorescence emission spectra of 0.025 g/L CuNC@MIP at different excitation wavelengths, H: fluorescence spectra of (0.025,0.05,0.075,0.1,0.125,0.15,0.175) g/L CuNC@MIP, I: fluorescence emission spectra of 0.01 g/L MIP at different excitation wavelengths, J: fluorescence spectra of (0.025,0.05,0.075,0.1,0.125,0.15,0.175) g/L MIP, K: fluorescence emission spectra of 0.0333 mmol/L CuNC at different excitation wavelengths, L: fluorescence spectra of (0.0333,0.08325,0.11655,0.1665,0.1998,0.24975,0.333) mmol/L CuNC, M: Infrared spectra of CuNC@MIP/MIP/CuNC.

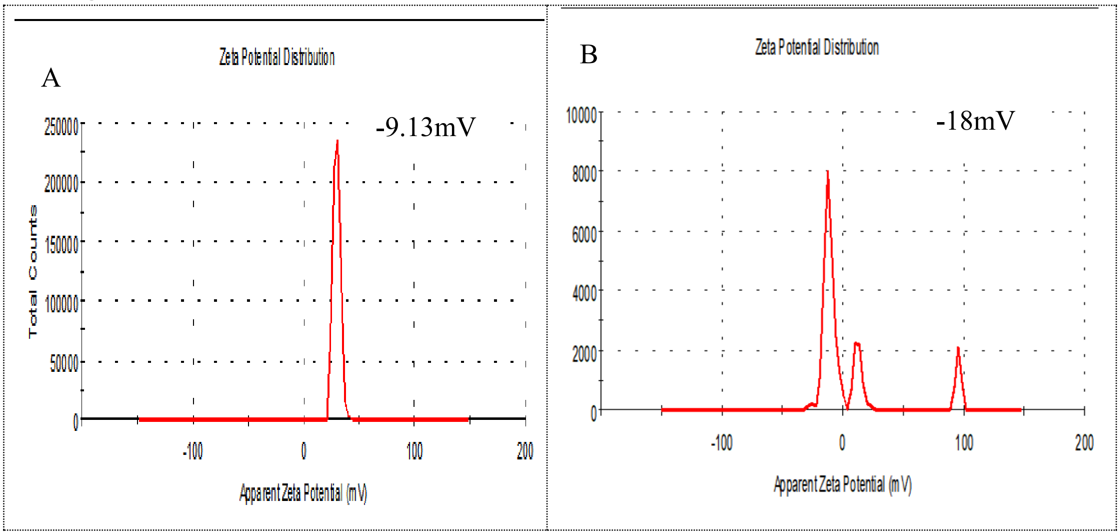

Fig. S3 Zeta potentials of CuNC@MIP and MIP

A: the Zeta potential of the CuNC@MIP, B: the Zeta potential of the MIP.

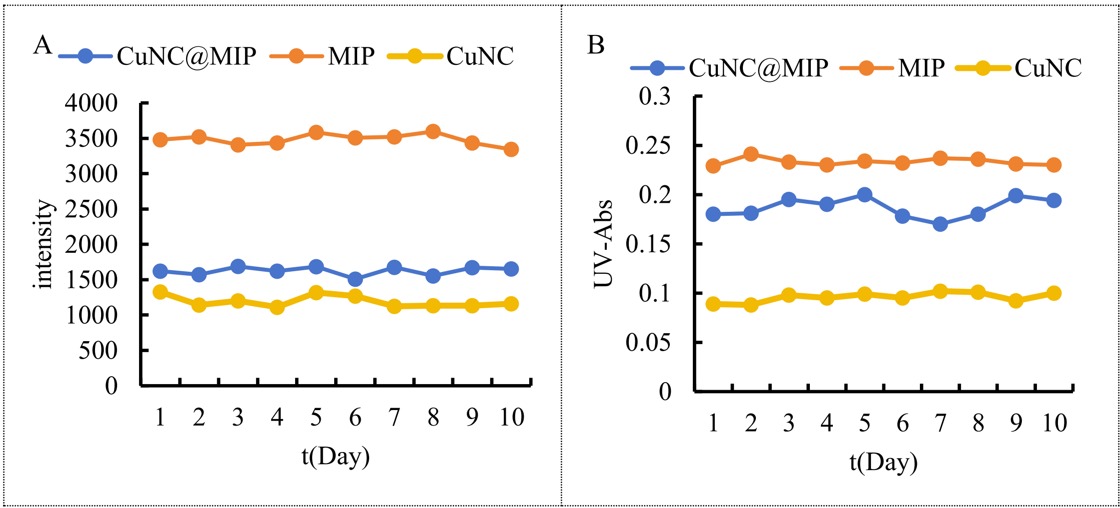

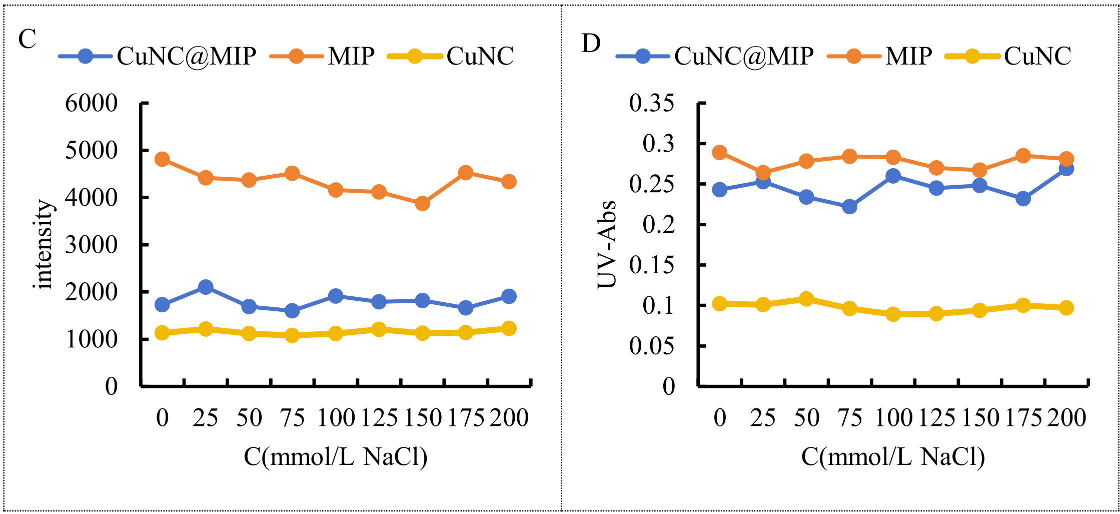

Fig. S4 Stability of CuNC@MIP, MIP, and CuNC at different times and in the NaCl solution A: RRS spectra of time stability of 0.1 g/L CuNC@MIP, 0.1 g/L MIP and 0.25 g/L CuNC, B: Abs spectra of time stability of 0.1 g/L CuNC@MIP, 0.1 g/L MIP and 0.25 g/L CuNC, C: RRS spectra of the stability of 0.1 g/L CuNC@MIP, 0.1 g/L MIP and 0.25 g/L CuNC in different concentrations of NaCl solutions；D: Abs spectra of the stability of 0.1 g/L CuNC@MIP, 0.1 g/L MIP and 0.25 g/L CuNC in different concentrations of NaCl solutions.

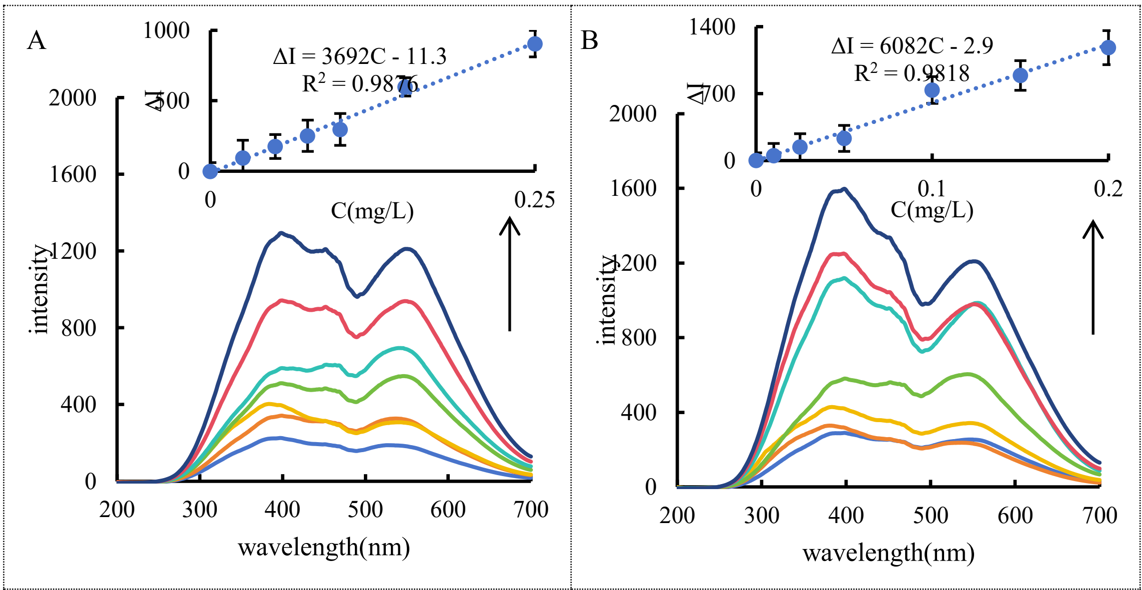

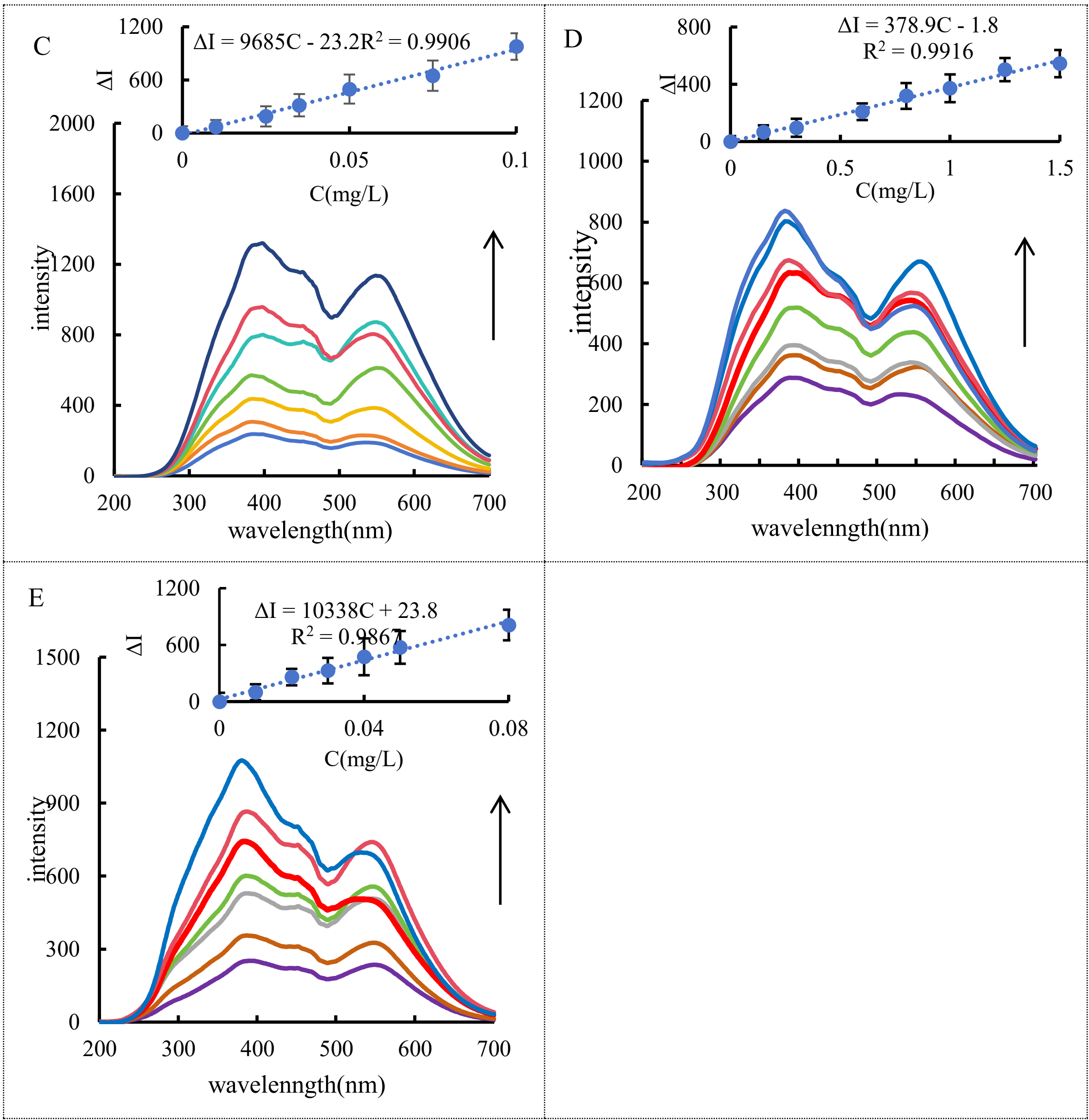

Fig. S5 RRS spectra of the AuNC@MIP/AgNC@MIP/CuNC/MIP/MIP/CuNC@MIP_{TCP} -$HAuCl_4$-hydrazine hydrate-HCl catalytic system (n=3)

A: (0,0.025,0.05,0.075,0.1,0.15,0.25) mg/L AuNC@MIP-0.04 g/L $HAuCl_4$- 0.10 mmol/L hydrazine hydrate-1.85 mmol/L HCl, B: (0,0.01,0.025,0.05,0.1,0.15,0.2) mg/L AgNC@MIP-0.04 g/L $HAuCl_4$-0.10 mmol/L hydrazine hydrate-1.85 mmol/L HCl, C: (0,0.01,0.025,0.035,0.05,0.075,0.1) mg/L CuNC@MIP- 0.04 g/L $HAuCl_4$-0.10 mmol/L hydrazine hydrate-1.85 mmol/L HCl, D: (0,0.15,0.3,0.6,0.8,1,1.25,1.5,1.75) mg/L MIP-0.04 g/L $HAuCl_4$-0.10 mmol/L hydrazine hydrate-1.85 mmol/L HCl, E: (0,0.01,0.02,0.03,0.04,0.05,0.08) mg/L CuNC@MIP_{TCP}-0.04 g/L $HAuCl_4$-0.10 mmol/L hydrazine hydrate-1.85 mmol/L HCl.

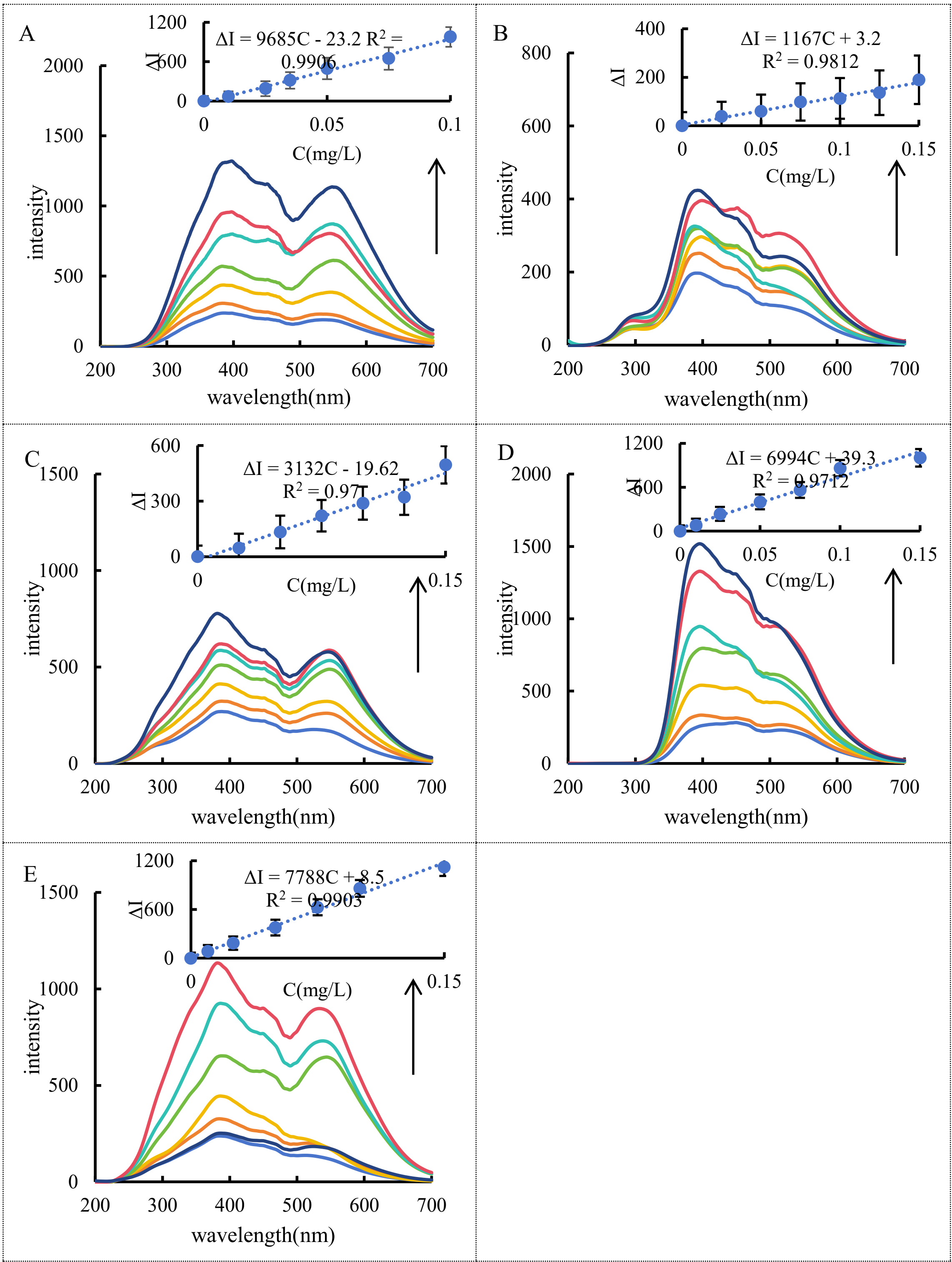

Fig. S6 RRS spectra of the CuNC@MIP-$HAuCl_4$-HCl-hydrazine hydrate/diphycarbazine/ hydroxylamine hydrochloride/sym-diphenylcarbazide/hydrazine sulfate catalytic system (n=3)

A: (0,0.01,0.025,0.035,0.05,0.075,0.1) mg/L CuNC@MIP-0.04 g/L $HAuCl_4$-0.10 mmol/L hydrazine hydrate-1.85 mmol/L HCl, B: (0,0.025,0.05,0.075,0.1,0.125,0.15) mg/L CuNC@MIP-0.04 g/L $HAuCl_4$-0.1 mmol/L diphenylcarbazone-1.85 mmol/L HCl, C: (0,0.025,0.05,0.075,0.1,0.125,0.15) mg/L CuNC@MIP-0.04 g/L $HAuCl_4$-7.5 mol/L hydroxylamine hydrochloride -1.85 mmol/L HCl, D: 0,0.01,0.025,0.05,0.075,0.1,0.15) mg/L CuNC@MIP-0.04 g/L $HAuCl_4$-10 mmol/L sym-diphenylcarbazide-1.85 mmol/L HCl, E:

(0,0.01,0.025,0.05,0.075,0.1,0.15) mg/L CuNC@MIP-0.04 g/L $HAuCl_4$-0.1 mmol/L hydrazine sulfate-1.85 mmol/L HCl.

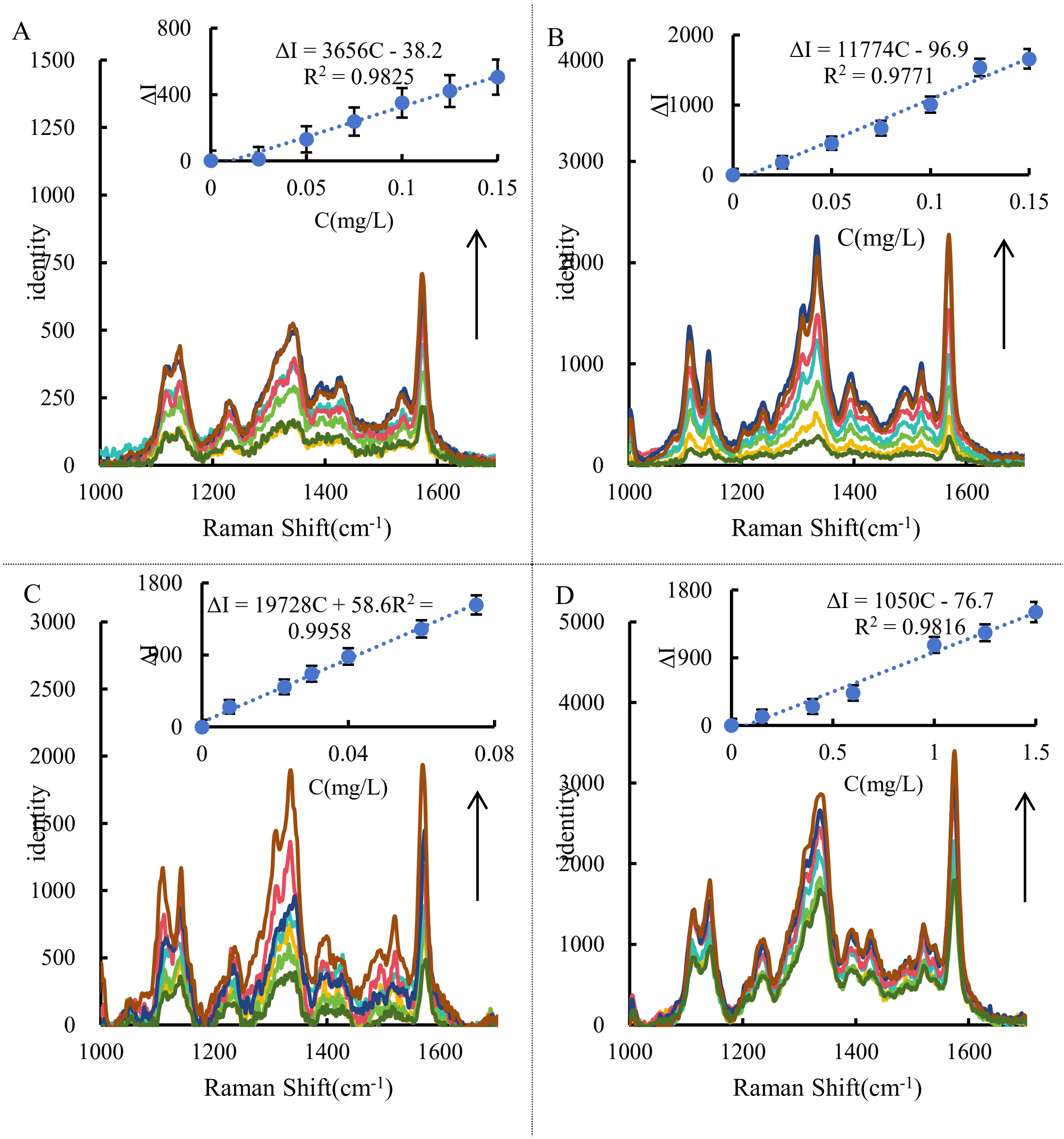

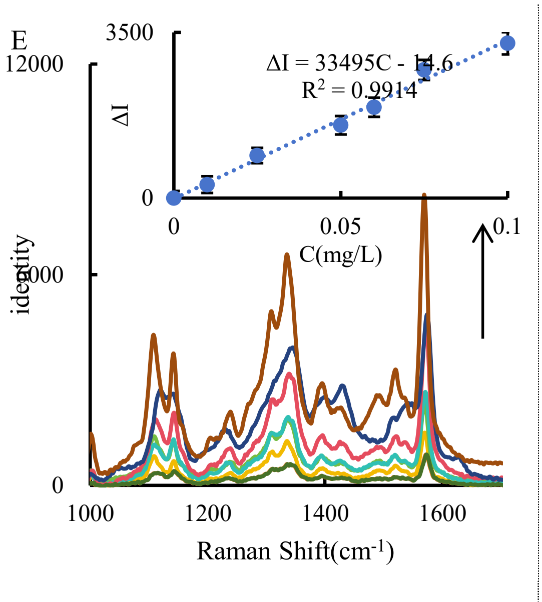

Fig. S7 SERS spectra of AuNC@MIP/AgNC@MIP/CuNC@MIP/MIP/CuNC@MIP_{TCP} -$HAuCl_4$-hydrazine hydrate-HCl catalyzed system (n=3)

A: (0,0.025,0.05,0.075,0.1,0.125,0.15) mg/L AuNC@MIP-0.04 g/L $HAuCl_4$-0.10 mmol/L hydrazine hydrate-0.5 mmol/L HCl-0.50 µmol/L VB4r, B: (0,0.025,0.05,0.075,0.1,0.125,0.15) mg/L AgNC@MIP-0.04 g/L $HAuCl_4$-0.10 mmol/L hydrazine hydrate-0.5 mmol/L HCl-0.50 µmol/L VB4r, C: (0,0.0075,0.0225,0.03,0.04,0.06,0.075) mg/L CuNC@MIP-0.04 g/L $HAuCl_4$-0.10 mmol/L hydrazine hydrate-1.85 mmol/L HCl-0.50 µmol/L VB4r, D: (0,0.15,0.4,0.6,1,1.25,1.5) mg/L MIP-0.04 g/L $HAuCl_4$-0.10 mmol/L hydrazine hydrate-1.85 mmol/L HCl-0.50 µmol/L VB4r, E: (0,0.01,0.025,0.05,0.06,0.075,0.1) mg/L CuNC@MIP_{TCP}-0.04 g/L $HAuCl_4$-0.10 mmol/L hydrazine hydrate-1.85 mmol/L HCl-0.50 µmol/L VB4r.

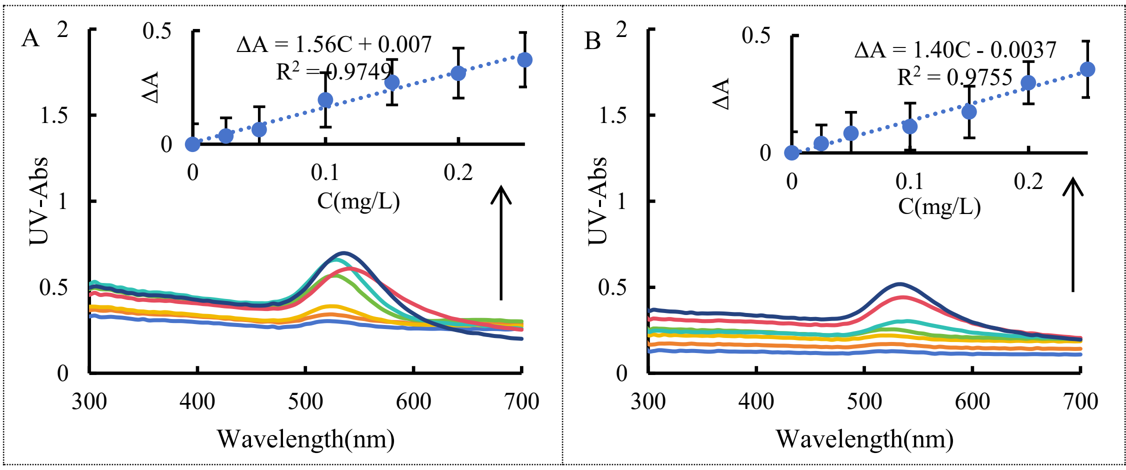

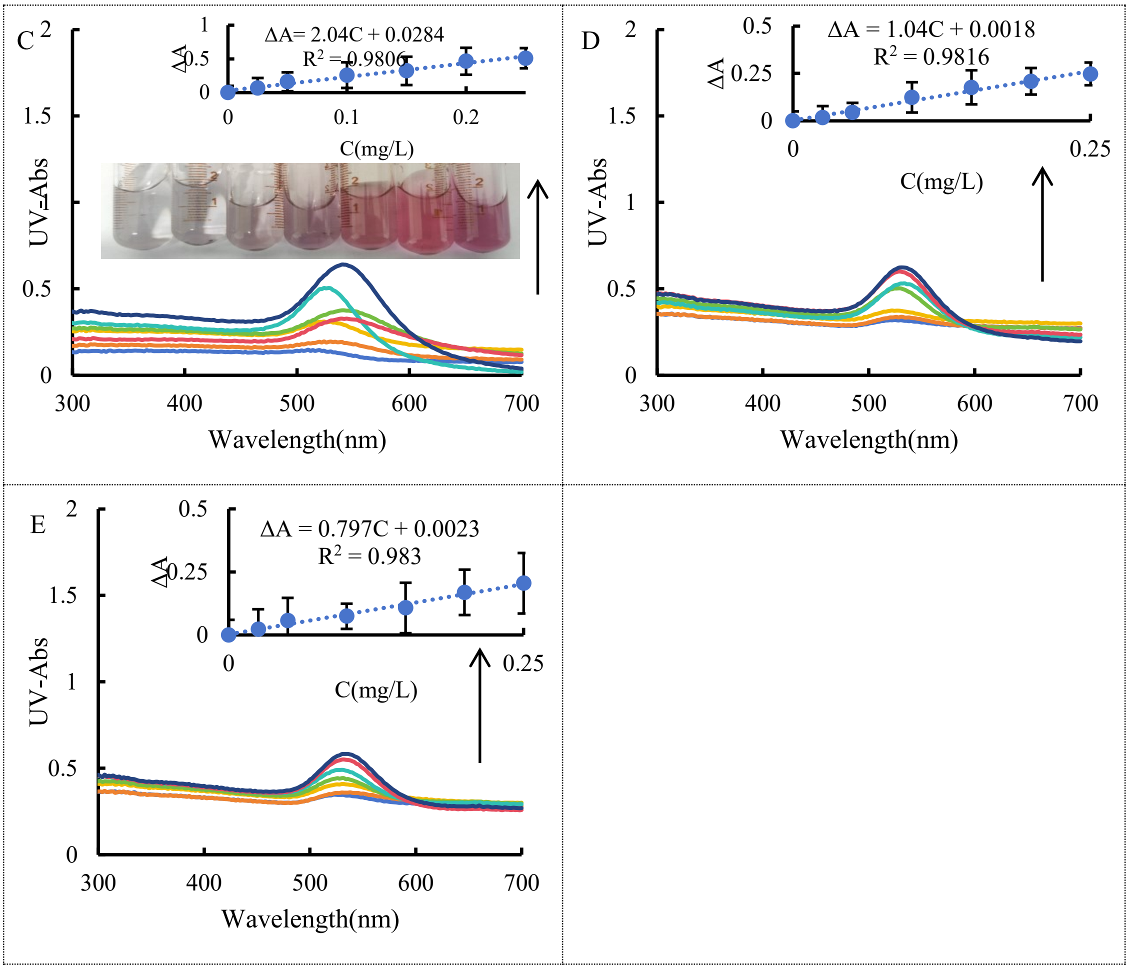

Fig. S8 UV spectra of AuNC@MIP/AgNC@MIP/CuNC@MIP/MIP/CuNC@MIP$_{TCP}$ -$HAuCl_4$-hydrazine hydrate-HCl catalytic system (n=3)

A: (0,0.025,0.05,0.1,0.15,0.2,0.25) mg/L AuNC@MIP-0.075 g/L $HAuCl_4$-0.45 mmol/L hydrazine hydrate-0.35 mmol/L HCl, B: (0,0.025,0.05,0.1,0.15,0.2,0.25) mg/L AgNC@MIP-0.075 g/L $HAuCl_4$-0.45 mmol/L hydrazine hydrate-0.35 mmol/L HCl, C: (0,0.025,0.05,0.1,0.15,0.2,0.25) mg/L CuNC@MIP-0.075 g/L $HAuCl_4$-0.45 mmol/L hydrazine hydrate-0.35 mmol/L HCl, D: (0,0.025,0.05,0.1,0.15,0.2,0.25) mg/L MIP-0.075 g/L $HAuCl_4$-0.45 mmol/L hydrazine hydrate-0.35 mmol/L HCl, E: (0,0.025,0.05,0.1,0.15,0.2,0.25) mg/L CuNC@MIP$_{TCP}$-0.075 g/L $HAuCl_4$-0.45 mmol/L hydrazine hydrate-0.35 mmol/L HCl.

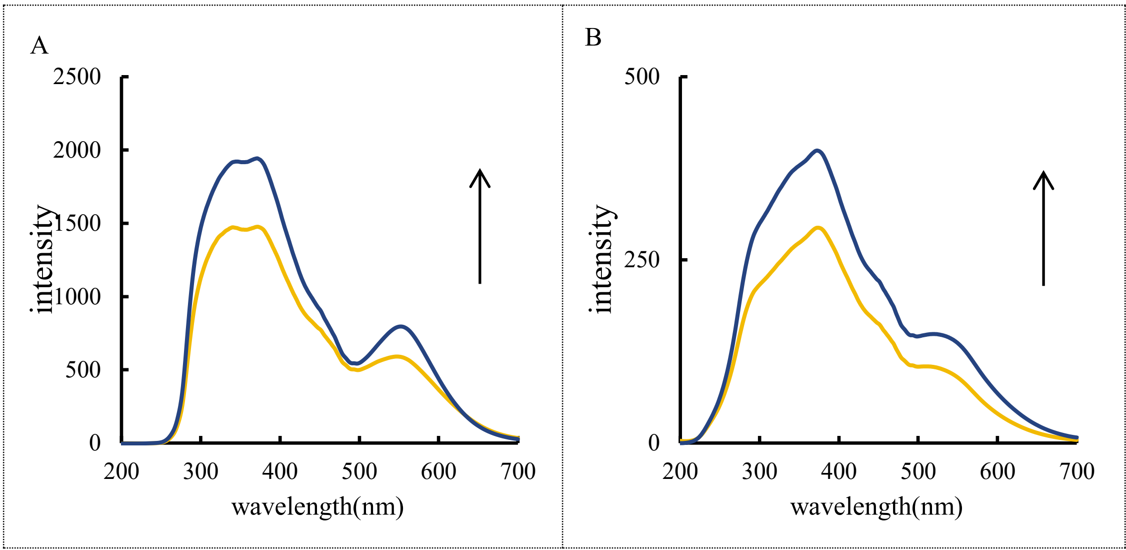

Fig.S9 RRS spectra of the tetraphenylborate/Au^{+} reaction systems

A: 0.04 mg/L CuNC@MIP- 0.04 g/L $HAuCl_4$-0.10 mmol/L hydrazine hydrate-1.85 mmol/L HCl-(0, 0.05) mmol/L sodium tetraphenylborate, B: (0, 0.08) mg/L CuNC@MIP- 0.04 g/L AuCl-0.10 mmol/L hydrazine hydrate.

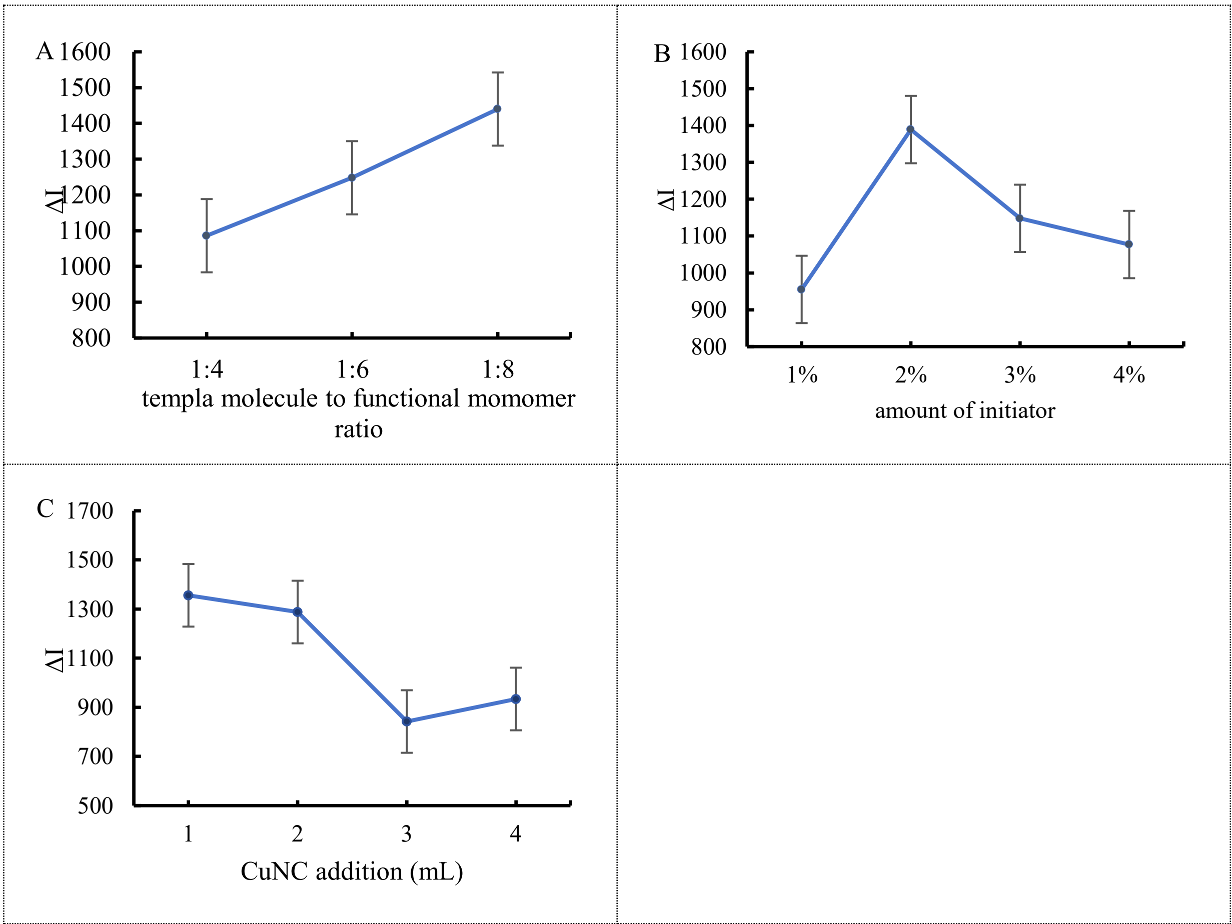

Fig. S10 Selection of the preparation conditions for the CuNC@MIP

A: effect of the amount of functional monomer used: 0.25 mmol TCP-(0.5, 0.085, 0.17) mL MAA-30 mL PVA-1.89 mL EGDMA-0.045 g AIBN-1 mL CuNC, B: effect of AIBN dosage: 0.25 mmol TCP-0.17 mL MAA-30 mL PVA-1.89 mL EGDMA-(0.022,0.045,0.065,0.087) g AIBN-1 mL CuNC, C: effect of the CuNC addition amount：0.25 mmol TCP-0.17 mL MAA-30 mL PVA-1.89 mL EGDMA-0.045 g AIBN-(1,2,3,4) mL CuNC.

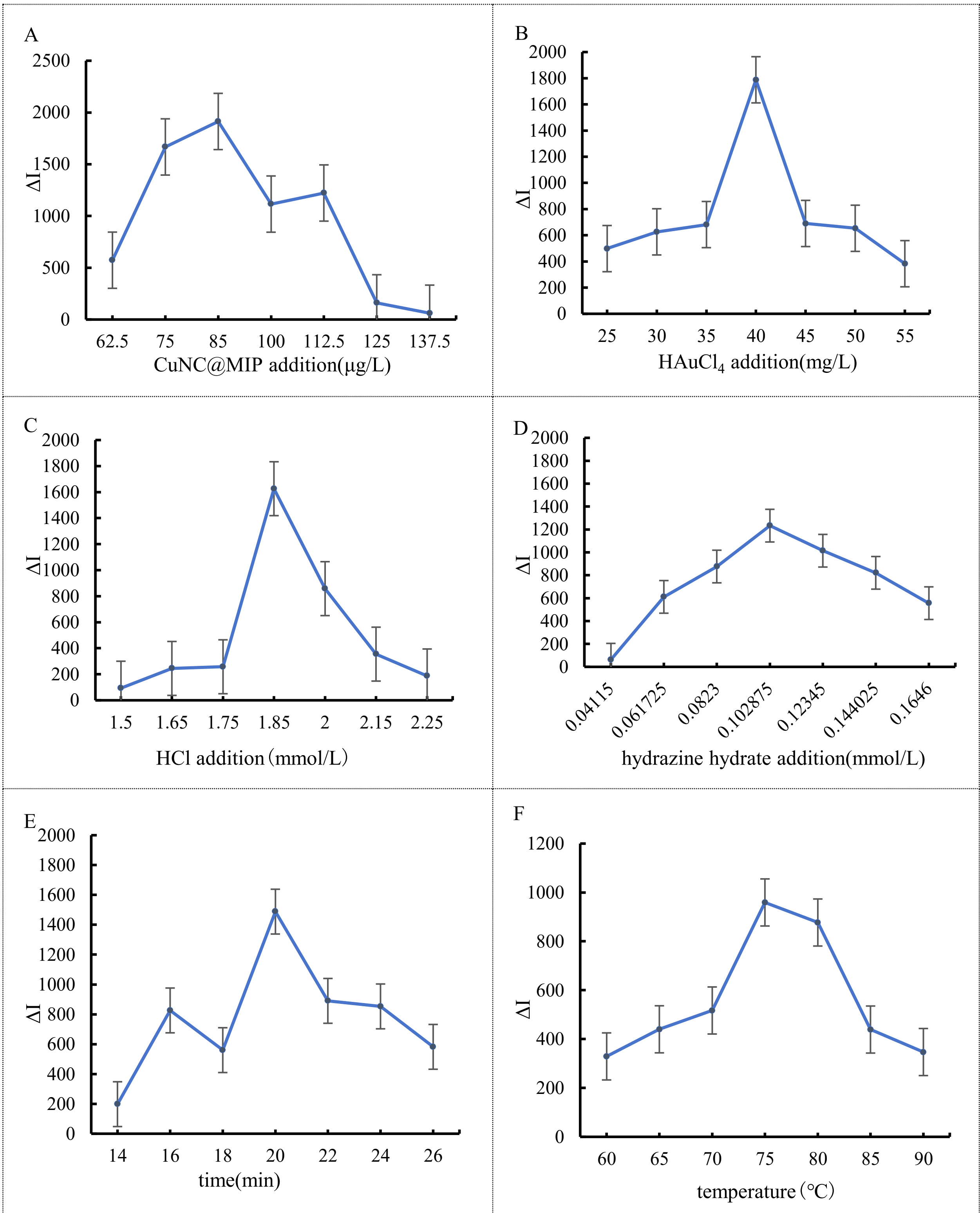

Fig. S11 RRS condition optimization for the CuNC@MIP-$HAuCl_4$-HCl-hydrazine hydrate assay system

A: effect of CuNC@MIP additions: CuNC@MIP(62.5,75,85,100,112.5,125,137.5) μg/L -0.0165 nmol/L TCP-40 mg/L $HAuCl_4$-1.85 mmol/L HCl-0.10 mmol/L hydrazine hydrate, 75 ℃ water bath 20 min, B: effect of $HAuCl_4$ additions: 85 μg/L CuNC@MIP-0.0165 nmol/L TCP-(25,30,35,40,45,50,55) mg/L $HAuCl_4$-1.85 mmol/L HCl-0.10 mmol/L hydrazine hydrate, 75 ℃ water bath 20 min, C: effect of HCl additions: 85 μg/L CuNC@MIP-0.0165 nmol/L TCP-40 mg/L $HAuCl_4$-(1.5,1.65,1.75,1.85,2,2.15,2.25) mmol/L HCl-0.10 mmol/L hydrazine hydrate, 75 ℃ water bath 20 min, D: effect of hydrazine hydrate additions: 85 μg/L CuNC@MIP-0.0165 nmol/L TCP-40 mg/L $HAuCl_4$-1.85 mmol/L HCl-(0.041,0.062,0.082,0.10,0.12,0.144,0.16) mmol/L hydrazine hydrate, 75 ℃ water bath 20 min, E: effect of time : 85 μg/L CuNC@MIP-0.0165 nmol/L TCP-40 mg/L $HAuCl_4$-1.85 mmol/L HCl-0.10 mmol/L hydrazine hydrate, 75 ℃ water bath (14,16,18,20,22,24,26) min, F: effect of temperature: 85 μg/L CuNC@MIP-0.0165 nmol/L TCP-40 mg/L $HAuCl_4$-1.85 mmol/L HCl-0.10 mmol/L hydrazine hydrate，(60,65,70,75,80,85,90) ℃ water bath 20 min.

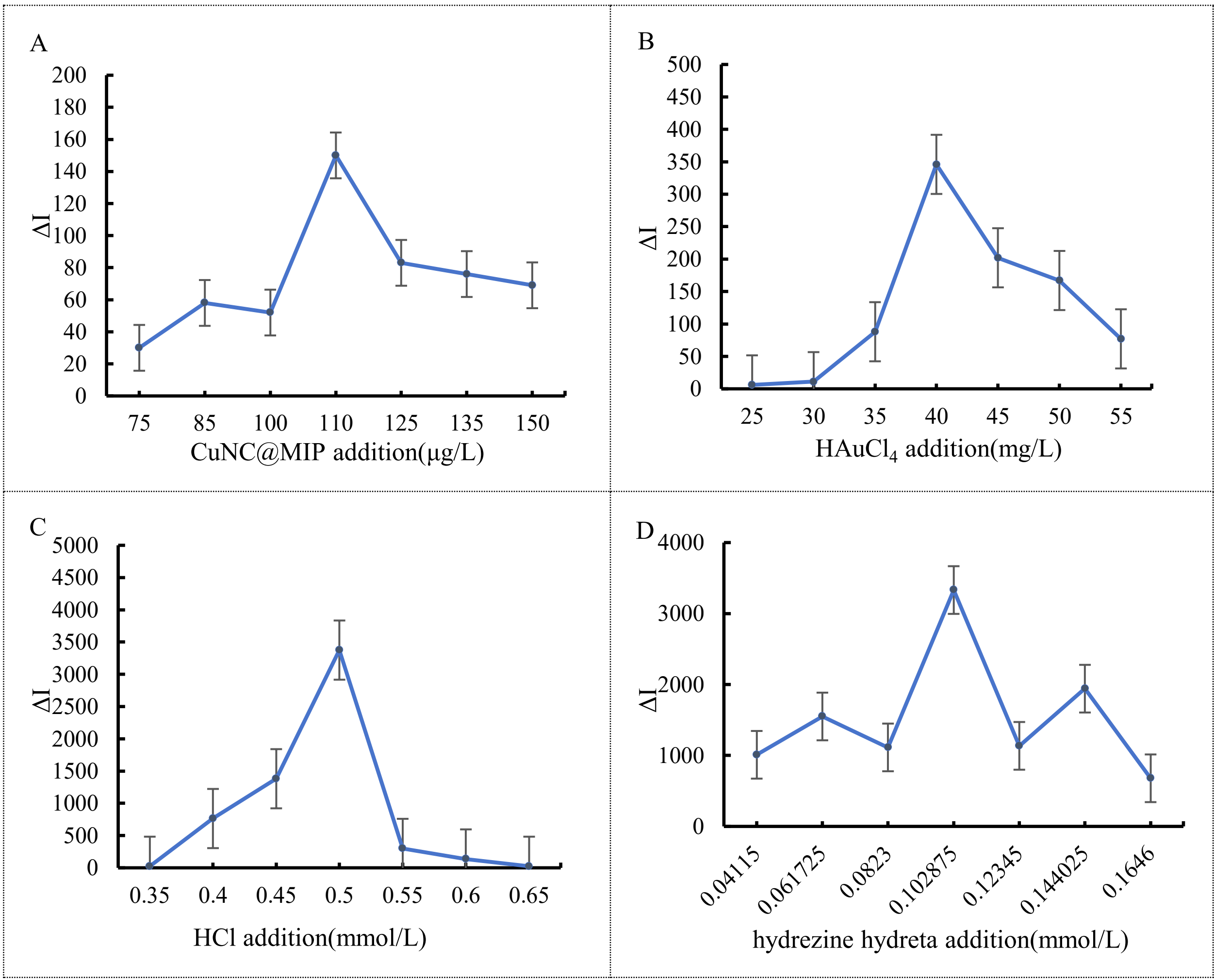

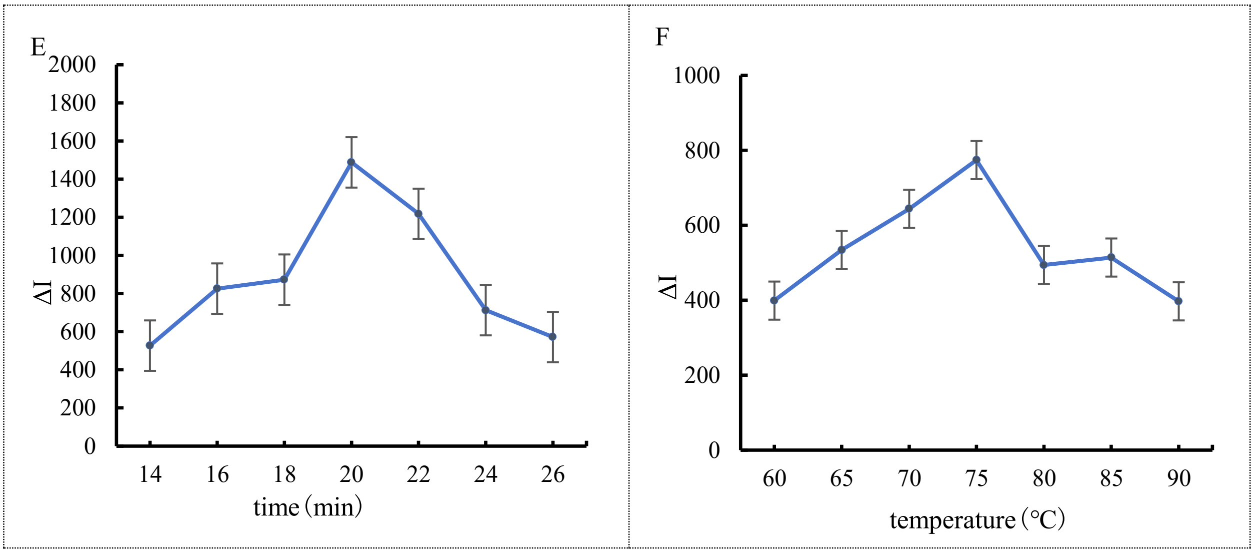

Fig. S12 CuNC @ MIPHAuCl$_4$-HCl-hydrazine hydrate analytical system

A: effect of CuNC@MIP additions: CuNC@MIP(75,85,100,110,125,135,150) μg/L -0.0165 nmol/L TCP-40 mg/L HAuCl$_4$-1.85 mmol/L HCl-0.10 mmol/L hydrazine hydrate, 75 ℃ water bath 20 min, B: effect of HAuCl$_4$ additions: 85 μg/L CuNC@MIP-0.0165 nmol/L TCP-(25,30,35,40,45,50,55) mg/L HAuCl$_4$-1.85 mmol/L HCl-0.10 mmol/L hydrazine hydrate, 75 ℃ water bath 20 min, C: effect of HCl additions: 85 μg/L CuNC@MIP-0.0165 nmol/L TCP-40 mg/L HAuCl$_4$-(0.35,0.4,0.45,0.5,0.55,0.6,0.65) mmol/L HCl-0.10 mmol/L hydrazine hydrate, 75 ℃ water bath 20 min, D: effect of hydrazine hydrate additions: 85 μg/L CuNC@MIP-0.0165 nmol/L TCP-40 mg/L HAuCl$_4$-1.85 mmol/L HCl-(0.041,0.062,0.082,0.10,0.12,0.144,0.16) mmol/L hydrazine hydrate, 75 ℃ water bath 20 min, E: effect of time : 85 μg/L CuNC@MIP-0.0165 nmol/L TCP-40 mg/L HAuCl$_4$-1.85 mmol/L HCl-0.10 mmol/L hydrazine hydrate, 75 ℃ water bath (14,16,18,20,22,24,26) min, F: effect of temperature: 85 μg/L CuNC@MIP-0.0165 nmol/L TCP-40 mg/L HAuCl$_4$-1.85 mmol/L HCl-0.10 mmol/L hydrazine hydrate，(60,65,70,75,80,85,90) ℃ water bath 20 min.

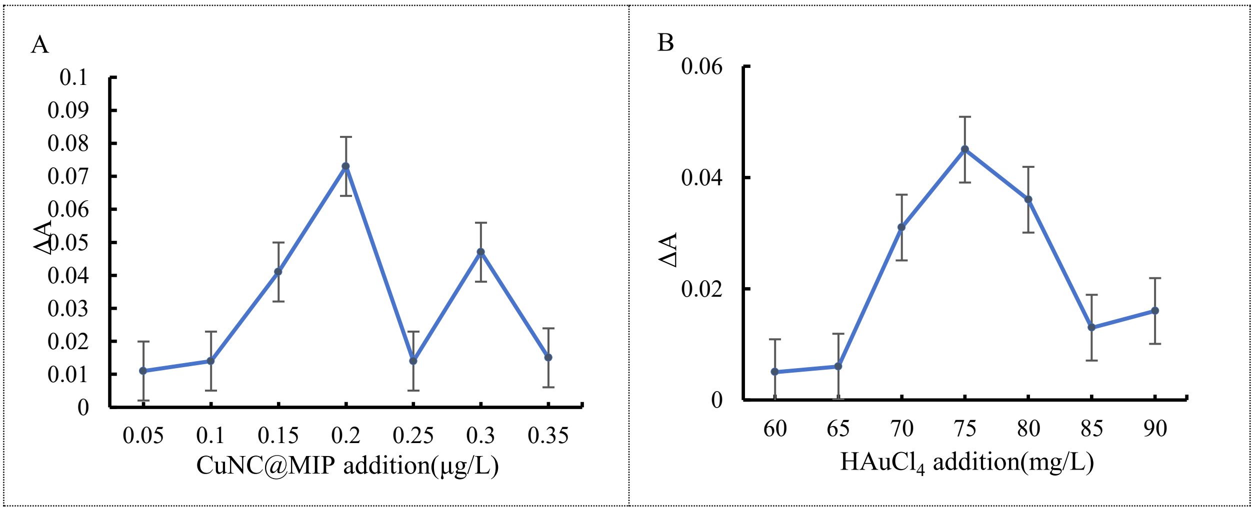

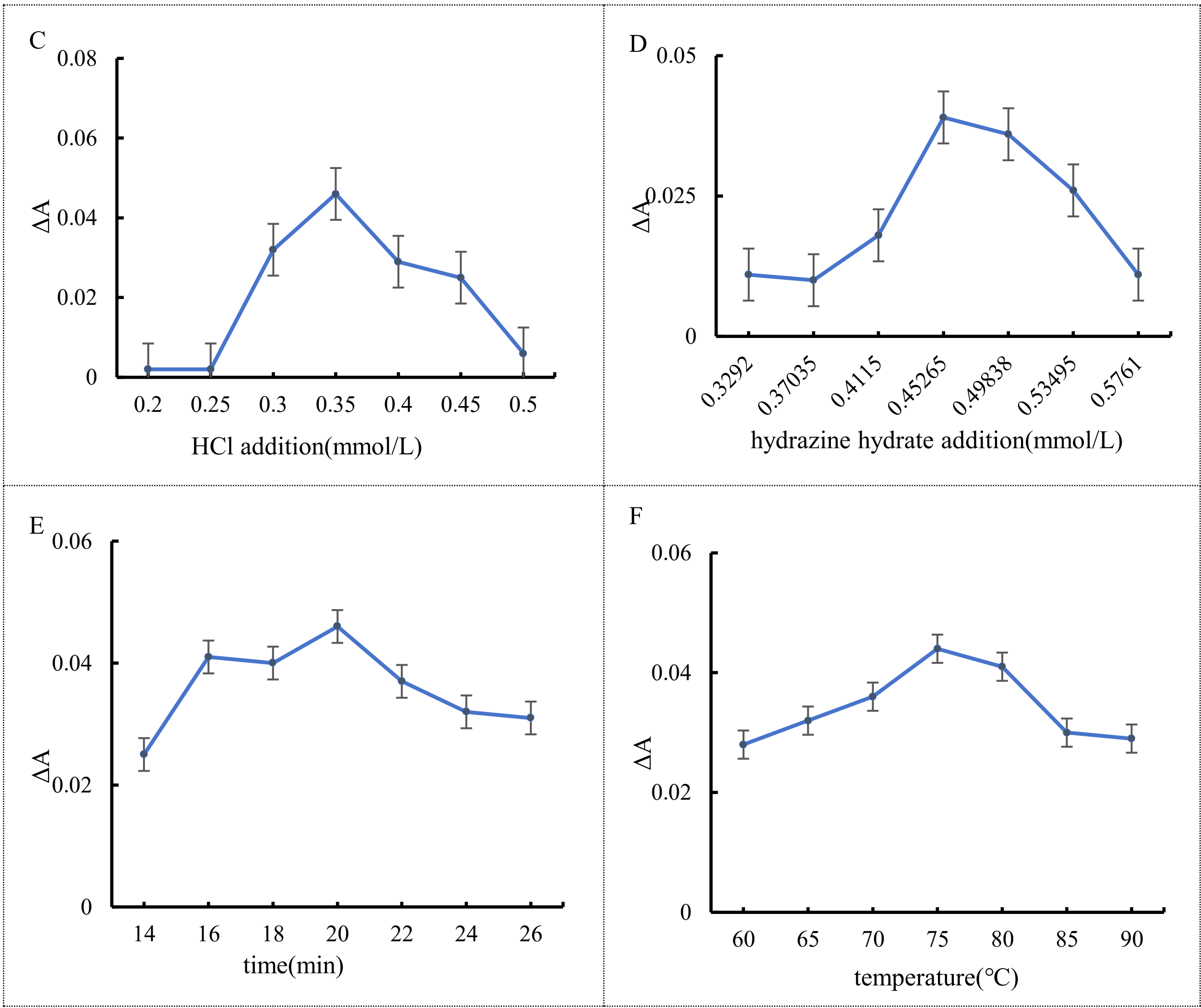

Fig S13.CuNC@MIP-$HAuCl_4$-HCl-hydrazine hydrate analysis system Abs condition optimization A: effect of CuNC@MIP additions: CuNC@MIP(0.05,0.1,0.15,0.2,0.25,0.3,0.35) mg/L -0.0165 nmol/L TCP-40 mg/L $HAuCl_4$-1.85 mmol/L HCl-0.10 mmol/L hydrazine hydrate, 75 ℃ water bath 20 min, B: effect of $HAuCl_4$ additions: 85 μg/L CuNC@MIP-0.0165 nmol/L TCP-(60,65,70,75,80,85,90) mg/L $HAuCl_4$-1.85 mmol/L HCl-0.10 mmol/L hydrazine hydrate, 75 ℃ water bath 20 min, C: effect of HCl additions: 85 μg/L CuNC@MIP-0.0165 nmol/L TCP-40 mg/L $HAuCl_4$-(0.2,0.25,0.3,0.35,0.4,0.45,0.5) mmol/L HCl-0.10 mmol/L hydrazine hydrate, 75 ℃ water bath 20 min, D: effect of hydrazine hydrate additions: 85 μg/L CuNC@MIP-0.0165 nmol/L TCP-40 mg/L $HAuCl_4$-1.85 mmol/L HCl-(0.33,0.37,0.41,0.45,0.49,0.53,0.58) mmol/L hydrazine hydrate, 75 ℃ water bath 20 min, E: effect of time : 85 μg/L CuNC@MIP-0.0165 nmol/L TCP-40 mg/L $HAuCl_4$-1.85 mmol/L HCl-0.10 mmol/L hydrazine hydrate, 75 ℃ water bath (14,16,18,20,22,24,26) min, F: effect of temperature: 85 μg/L CuNC@MIP-0.0165 nmol/L TCP-40 mg/L $HAuCl_4$-1.85 mmol/L HCl-0.10 mmol/L hydrazine hydrate,(60,65,70,75,80,85,90) ℃ water bath 20 min.

Table S1.CuNC@MIP-$HAuCl_4$-HCl-hydrazine hydrate/diphenylcarbazone/hydroxylamine hydrochloride/sym-diphenylcarbazide/hydrazine sulfate

reducing agent	linearity range (mg/L)	linear equation	correlation coefficient （R^2）

hydrazine hydrate	0.01-0.1	ΔI_{370nm}= 9690C - 23.2	0.9906
diphenylcarbazone	0.025-0.15	ΔI_{370nm}= 1167C + 3.2	0.9812
hydroxylamine hydrochloride	0.025-0.15	ΔI_{370nm}= 3132C - 19.6	0.9700
sym-diphenylcarbazide	0.01-0.15	ΔI_{370nm}= 6994.3C +8.5	0.9712
hydrazine sulfate	0.01-0.15	ΔI_{370nm}= 7787.9C+ 11.3	0.9903

Table S2. Comparison of the catalytic properties of the nanomaterials

material	linearity range (mg/L)	linear equation	correlation coefficient （R^2）
AuNC@MIP	0.025-0.25	$\Delta I_{370nm} = 3.69\times10^3 C_{AuNC@MIP}$ - 11.3	0.9876
AuNC@MIP	$5x10^{-7}$-$4.5x10^{-5}$	$\Delta I_{370nm}= 2.17\times10^7 C_{AuNC}$ - 11.3	0.9900
AgNC@MIP	0.01-0.2	$\Delta I_{370nm}= 6.08\times10^3 C_{AgNC@MIP}$ - 2.9	0.9818
AgNC@MIP	$8.19x10^{-6}$-$1.638x10^{-4}$	$\Delta I_{370nm}= 7.42\times10^6\ C_{AgNC}$ - 2.9	0.9800
CuNC@MIP	0.01-0.1	$\Delta I_{370nm}= 9.69\times10^3 C_{CuNC@MIP}$ - 23.2	0.9906
CuNC@MIP	$1.23x10^{-5}$-$1.23x10^{-4}$	$\Delta I_{370nm}=7.87\times10^6 C_{CuNC}$ - 23.2	0.9900
CuNC@NIP	0.1-1	$\Delta I_{370nm}= 3.61\times10^2 C_{CuNC@NIP}$ - 8.4	0.9859
CuNC@NIP	$1.23x10^{-4}$-$1.23x10^{-3}$	$\Delta I_{370nm}= 2.00\times10^5 C_{CuNC}$ - 8.4	0.9859
$CuNC@MIP_{TCP}$	0.01-0.075	$\Delta I_{370nm}= 1.00\times10^4 C_{CuNC@MIPTCP}$ + 23.8	0.9867
$CuNC@MIP_{TCP}$	$1.47x10^{-5}$-$1.305x10^{-4}$	$\Delta I_{370nm}= 6.00\times10^6 C_{CuNC@MIPTCP}$ + 23.8	0.9900
MIP	0.2-1.75	$\Delta I_{370nm}= 378.86 C_{MIP}$ - 1.8	0.9916
AuNC	0.01-0.075	$\Delta I_{370nm}= 1006.9 C_{AuNC}$ + 27.3	0.9727
AgNC	0.01-0.08	$\Delta I_{370nm}= 1008 C_{AgNC}$ - 6.6	0.9833
CuNC	0.042-0.026	$\Delta I_{370nm}= 1300.8 C_{CuNC}$ - 46.7	0.9937

Table S3.Comparison of the reported assays for the determination of TCP

Method	Method principle	Linearity range (nmol/L)	LOD (nmol/L)	Annotation	reference
Electrochemical process	A graphite carbon nitride nanosheet with Fe_3O_4 nanorods ($CN@Fe_3O_4$) composite modified screen-printed carbon electrode (SPCE) was prepared as a novel selective electrochemical sensor for the detection of TCP.	4×10^{-5}-0.651	12	High selectivity and complex sensor preparation	[42]

phosphorescence	A magnetic molecularly imprinted phosphorescent nanoparticle probe doped with quantum dots (QDs) using TCP as a template molecule and Fe_3O_4 as a core was prepared. Due to the presence of QDs, good magnetic properties and high selectivity for TCP, the resulting nanoprobe shows intense phosphorescence.	1×10^2-3×10^4	35	Highly selective, complex probe preparation	[43]
Fluorescence	An ideal fluorescent MIP sensor SiO2@dye-MIP with TCP as a template, 7-allyloxycoumarin as a fluorescent functional monomer, and 3-(methacryloyloxy)propyl trimethoxysilane (MPS)-modified SiO2 spheres as a solid carrier has been designed, which selectively detects TCP by solid-state fluorescence detection without dispersive solution.	1-1000	0.53	Simple operation and wide linear range	[44]
HPLC-UV	Covalent triazine skeletons (CTFs) were introduced into stir bar sorptive extraction (SBSE) and polydimethylsiloxane (PDMS)/ CTFs stir bar coatings were prepared by sol-gel technique for the adsorption of TCP followed by high performance liquid chromatography-ultraviolet (HPLC-UV) detection.	5-2538	1.47	Wide linear range, high extraction efficiency, complex operation	[47]

Gas chromatography	Simultaneous dispersive liquid-liquid microextraction and derivatization methods based on low-density solvents for the simultaneous determination of chloroanisole and TCP in water.	0.0508-50.8	0.015	Efficient and simple, low sensitivity	[48]
Microorganisms - Gas Chromatography	Quantitative conversion of TCP to 2,4,6-trichloroanisole (TCA) using microorganisms, followed by detection and analysis of TCA by gas chromatographyTCP	0.508-50.8	0.026	High selectivity and complex operation	[49]
RRS/SERS/Abs	Based on the catalytic amplification and recognition function of CuNC@MIP, AuNP was used as an indicator to determine TCP.	0.01-0.1 7.5×10^{-3}-7.5×10^{-2} 0.01-0.1	0.021 0.0010 0.042	High sensitivity, good selectivity, easy to operate	This work

Table S4. Effect of coexisting substances on the determination of TCP by RRS

Coexisting substances	Factor	Fractional error（%）	Coexisting substances	Factor	Fractional error（%）
Phenol	100	-5.45	K^{+}	1000	1.73
4-Chlorophenol	100	-2.48	Al^{3+}	1000	-3.00
Bisphenol A	400	-2.21	Hg^{2+}	1000	-1.13
catechol	400	2.21	Mn^{2+}	1000	1.15
atrazine	400	2.85	I^{-}	1000	2.52
Cu^{2+}	1000	6.12	Mg^{2+}	1000	-6.89
NH^{4+}	1000	-8.19	SO_3^{2-}	1000	-3.12
Ca^{2+}	1000	-0.74	CO_3^{2-}	1000	-5.61
Na^{+}	1000	-3.1	Cr^{3+}	1000	1.10
Fe^{3+}	1000	-9.4	F^{-}	1000	1.66

NO_3^-	1000	3.10	Cd^{2+}	1000	1.94

Table S5. Measurement of TCP in water samples

Sample	Average (nmol/L)	Added (nmol/L)	Found (nmol/L)	Recovery (%)	RSD (%)	Content (nmol/L)
Domestic wastewater 1	0.027	0.005	0.032	97.223	1.115	0.0534
Domestic wastewater 2	0.027		0.032	108.561	1.700	0.0537
Domestic wastewater 3	0.027		0.033	102.892	1.438	0.0548
Tap water 1	0.022		0.027	97.873	0.566	0.0447
Tap water 2	0.021		0.025	94.611	2.522	0.0415
Tap water 3	0.021		0.026	101.936	0.587	0.0427
Rainwater 1	0.023		0.028	97.987	0.946	0.0463
Rainwater 2	0.024		0.029	107.287	0.770	0.0480
Rainwater 3	0.023		0.028	100.854	0.505	0.0451
Lake water 1	0.025		0.030	98.497	1.431	0.0501
Lake water 2	0.023		0.028	97.860	0.468	0.0457
Lake water 3	0.021		0.026	98.751	1.001	0.0417